LUPINE PUBLISHERS

ISSN: 2832-5230

Open Access Journal of Bio-sensors & Renewable sources

DOI: 10.32474/JBRS.2022.02.000134

Research Article

Evaluating the Weather Research and Forecasting model to predict Wind Speed over Egypt, Sudan, and South Sudan

Gamal El Afandi[1]*, Mostafa Morsy[2] and Hossam Ismael[1,3]

[1]*College of Agriculture, Environment and Nutrition Sciences, Tuskegee University, USA*

[2]*Astronomy and Meteorology Department, Faculty of Science, Al-Azhar University, Egypt*

[3]*Department of Geography & GIS, Faculty of Arts, New Valley University, Egypt*

***Corresponding author:** Gamal El Afandi, College of Agriculture, Environment and Nutrition Sciences, Tuskegee University, Tuskegee, AL 36088, USA

Received: December 02, 2022 **Published:** December 15, 2022

Abstract

The wind is one of the main significant renewable energy resources not only for developing countries but also all over the globe. It could be used to overcome the increasing energy power demand in many countries, especially Egypt, Sudan, and South Sudan. In addition, it is a good source of clean energy that could be used to reduce air pollution in these countries. The main objective of this research is to evaluate the performance of the Weather Research and Forecasting (WRF) model to predict wind speed over Egypt, Sudan, and South Sudan. Nineteen weather stations were selected from the three countries for this purpose. Therefore, the statistical parameters of the Willmott Index of agreement (WI), Coefficient of Determination (R2), Normalized Root Mean Square Error (NRMSE), and Normalized Mean Bias Error (NMBE) were used in the evaluation processes. The results revealed that the WRF performance was high during autumn and winter in Egypt, Sudan, and South Sudan, while it was low during summer in all countries. In addition, strong correlations were found between measured and forecasted wind speeds for the selected days during all seasons. At the same time, WI and R2 values were approximately close to 1, while NRMSE and NMBE were approaching zero. Therefore, there is no significant difference between the real and forecasted wind speeds during all seasons. Overall results proved the capability of the model to predict wind speed over Egypt, Sudan, and South Sudan compared to measurements. Therefore, it may conclude that all countries could depend on the WRF model to predict wind speed in the past, present, and future with high accuracy.

Keyword: Wind speed; WRF model evaluation; statistical indicators

Introduction

The wind is one of the most important determinants of the climatic conditions that shape weather systems over different regions of the earth's surface [1]. Its first role and responsibility are transporting energy, momentum, and moisture horizontally and vertically in the atmosphere [2]. For example, the wind is carrying air masses and pollutants and disperses them from place to place on the Earth's surface [3,4]. The earth's surface heating and cooling because of an uneven geographical distribution of solar radiation incidence on the surface leads to pressure gradient forces, which in turn leads to winds. As a result, the evolution of horizontal pressure gradients, which are kept constant by the Coriolis force of the earth's rotation, is the principal cause of air motion [5]. The atmosphere balances the uneven distribution of pressure and radiation (heating and cooling) over the surface of the Earth through winds. Wind resource assessment can be divided into two steps; a regional wind assessment, which evaluates the resources of

a region as a first approach, and a site-specific assessment, which is a detailed evaluation of specific areas that exhibit high potential in the regional assessment [6].

The regional wind assessment is mostly based on numerical weather prediction (NWP) models [7-9]. Due to the high spread of wind power in the electricity system, the accuracy of wind prediction systems becomes increasingly important [10,11], have indicated that accurate wind forecasting is an essential process for modern electrical networks. In addition, a small error or little change in the accuracy of the wind speed forecast can reflect a high error in the wind power forecast [12,13], where the wind power is proportional to the cube of the wind velocity. Therefore, accurate wind forecasts save billions of dollars per year. In the absence or scarcity of wind speed measurements, alternative techniques and methods are required to assess and estimate wind resource availability, one of the most important studies in this application was performed by [14,15]. It should provide, at a minimum, an accurate average wind speed and power density prediction to better estimate the annual energy production [16]. The scaling techniques typically estimate the average wind speeds, while the power density can be estimated using the distribution of site wind speed [17]. Numerical Weather Prediction (NWP) datasets for wind speed are available in several resolutions and heights but must be scaled to provide more accurate near-surface wind speed [18].

Current NWP models resolve several local and regional circulation patterns, considering local topographic surface features to a certain extent. Thus, these models can provide accurate information for meteorological parameters, such as wind speed and direction, over large regions at high temporal and spatial resolution [19]. Predicting wind speed is a challenging task due to its inherent characteristics such as non-linearity and randomness. Modern NWP models have adopted sophisticated microphysics schemes that can depict the fine-scale atmospheric processes affecting heat, moisture, and momentum transfers. NWP models take into consideration the effects of the earth's surface features and properties. These features have substantial effects on local weather characteristics, especially within the mixed boundary layer. The use of NWP data scaled by the boundary layer scaling (BLS) model could offer improved near-surface wind speed and power density predictions compared to the use of the reference datasets [20]. Three dimensions weather simulations can provide detailed descriptions of atmospheric motions occurring over complex mountainous terrains [21]. Limited-area high-resolution NWP models can deliver good wind estimates in an approximately temporal range of 6 hours out to 6 days [22]. High-resolution nested models can describe fine-scale atmospheric phenomena, and their results have gradually become competitive with synoptic observations.

Non-hydrostatic weather forecasting models using nesting runs can supply good estimates of the wind conditions at local and simple synoptic scales when their results are compared to wind measurements [23]. Many numerical studies of wind resource assessment in different regions have compared the estimated wind velocity with the measured ones, and the comparisons showed a good agreement [24,25]. Increasing the resolution of numerical simulations along with the three-dimensionality representation of the topography can improve the model solution [26]. In recent years, many scientists have conducted a lot of research on the prediction of wind power. The Weather Research and Forecasting (WRF) model is one of the most widely used NWP models and is a reference for regional wind resource assessment [27,28]. The estimation of wind speed at 60 m (which is typically the height of the turbine hub) with the high horizontal resolution has been analysed by coupling of WRF mesoscale model and the Wind Atlas Analysis and Application Program (WASP) micro-scale model [29]. Also, the WRF model produces good results in wind speed predictions at 60 m in comparison to Final Analysis (FNL) wind speed data at 10 m using power law in Tanzania [30].

Several studies indicated that the configuration and scheme selection into the NWP model for wind simulation is region-dependent [31-35]. In a while, the initial and lateral boundary conditions, the model spin-up time [36,37], the parameterization of the influence of turbulence on wind velocity components [38] and planetary boundary layer (PBL) schemes [39] are the main dependant factors for the low-level wind's accurate simulation at high resolutions in the NWP models. Therefore, a set of configurations in the NWP model must be determined for mapping the spatial wind resources [40,41] studied the effect of four modifications to the WRF model during eight simulation experiments. The modifications included Radio occultation data assimilation, different versions of the WRF model, utilizing bulk microphysics schemes that have been established in the period from 1983 to 2011, and completely coupling WRF to the ocean dynamic model. The accuracy of the simulation has been evaluated through a comparison between each simulation to the Global Forecasting System (GFS) model analysis [42], studied the evaluation of non-convective wind forecasting methods in the 15th operational weather squadron area of responsibility.

The study assessed two different techniques for forecasting non-convective wind gusts at different five positions. Using a WRF ensemble data set, the results indicated that the Rapid Update Cycle's wind gust algorithm (RUC) led to a better performance at three of the five locations when evaluated with more than the 35-knot threshold. The results of this study indicated that integration between two non-convective wind-gust prediction techniques into operational forecasts at the 15th operational weather squadron could give better accuracy with more evaluation and testing against other accepted techniques. The spatial and temporal high-resolution of wind velocity observations are insufficient in Egypt, Sudan, and South Sudan. Hence, they could overcome this problem using numerical weather prediction models. The wind-energy resource evaluation needs long historical wind speed and direction observations. The observed wind data are not adequate to study the national wind resource over Egypt, Sudan, and South Sudan. This study proposed to use the WRF model, as one of the

new-generation numerical weather prediction models that include advanced dynamics, physics, and numerical schemes and is suitable for a broad spectrum of applications across scales ranging from meters to thousands of kilometres. The basic reason for selecting the WRF model is its dynamic core, the physical framework, and the software framework. The major goal of this study is to evaluate regionally the performance and effectiveness of the WRF model in predicting wind over Egypt, Sudan, and South Sudan to confirm its capacity to provide accurate wind data in comparison to observations.

Materials and Methods

Study Region and Stations

Egypt, Sudan, and South Sudan are located in the northeast of Africa, and they are bounded by latitudes from 3 to 32°N and longitudes from 21 to 39°E. The study area with plotted weather stations (ten in Egypt and nine in Sudan and South Sudan) is shown in Figure 1. The detailed geographical information for the selected stations is presented in Tables 1 & 2.

Figure 1: Study area with the selected weather stations in Egypt, Sudan, and South Sudan.

Table 1: Egypt stations, their IDs, latitudes, longitudes, elevations, and WMO numbers.

Station	Country	ID	Lat. (°N)	Lon. (°E)	Elev. (m)	WMO
Mersa Matruh	EG	HEMM	31.33	27.22	30	62306
Alexandria	EG	HEAX	31.2	29.95	7	62318
Port Said	EG	HEPS	31.28	32.23	6	62332
Cairo	EG	HECA	30.13	31.4	74	62366
Menia	EG	HEAM	28.08	30.73	40	62387
Aswan	EG	HESN	23.97	32.78	194	62414
Siwa	EG	-	29.2	25.32	-13	62417
Dakhela	EG	-	25.48	29	111	62432
El Tor	EG	HETR	28.21	33.64	21	62459
Kosseir	EG	-	26.13	34.15	11	62465

Table 2: Sudan and South Sudan stations, their IDs, latitudes, longitudes, elevations, and WMO numbers.

Station	Country	ID	Lat. (°N)	Lon. (°E)	Elev. (m)	WMO
WadiHalfa	SU	HSSW	21.82	31.48	183	62600
Abu Hamed	SU	-	19.53	33.32	312	62640

Port Sudan	SU	HSSP	19.58	37.22	3	62641
Karima	SU	-	18.55	31.85	249	62660
Atbara	SU	HSAT	17.70	33.97	347	62680
Kassala	SU	HSKA	15.47	36.40	500	62730
El Fasher	SU	HSFS	13.62	25.33	733	62760
El Obeid	SU	HSOB	13.17	30.23	574	62771
Juba	SSU	HSSJ	4.87	31.60	460	62941

Data and Methodology

The Advanced Research Weather Research and Forecasting (WRF-ARW) model version 3.8.1 is used to perform three-dimensional real-time high-resolution nested experiments to estimate the wind speed over the two countries. The six-hourly reanalysis datasets from (i) the National Centre for Environmental Prediction/National Centre of Atmospheric Research (NCEP/NCAR) with 2.5° X 2.5° spatial resolution and 18 vertical pressure levels; and (ii) from the Global Forecast System Final Analysis (GFS-FNL) with 1°x1° horizontal resolution and 27 vertical pressure levels are used as the initial and lateral boundary conditions to run WRF model. In addition, the observed wind speed data is collected from the selected 19 ground stations inside Egypt, Sudan, and South Sudan and used to evaluate the WRF model performance for wind prediction. During this study, the WRF model is run on three nest domains with horizontal resolutions of 30 km (Domain one, DM1), 10 km (Domain 2, DM2), and 3 km (Domain 3, DM3) using the two-way nesting option. The third nested domain (DM3) of 3 km grid spacing is centered on the study area (Egypt, Sudan, and South Sudan, Figure 2 and used as the main output to achieve the purposes of this research.

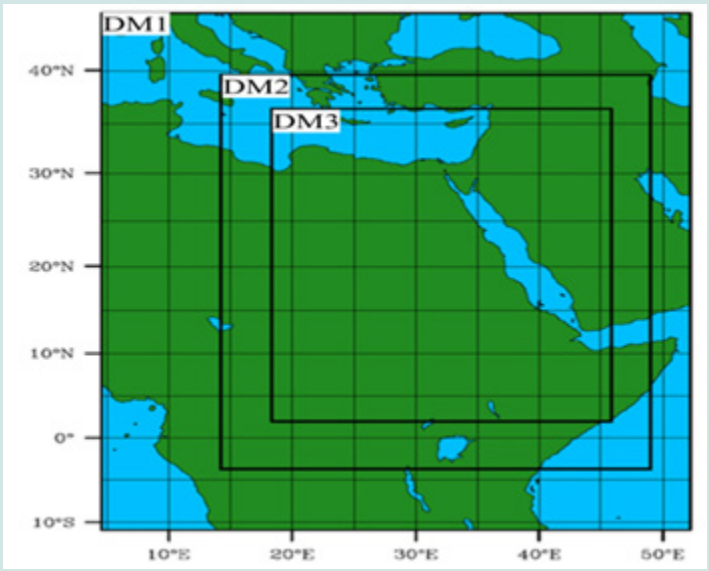

Figure 2: WRF model domains of 30 km (DM1), 10 km (DM2), and 3 km (DM3) horizontal resolution.

By applying some statistical analysis and procedures on the observed wind speed data at the selected stations in Egypt, Sudan, and South Sudan during the period 1981-2010, it is found that the days of 22 January 2010, 26 April 1999, 12 September 1989, and 7 November 2003 contain the maximum wind speed in winter, spring, summer, and autumn respectively. Accordingly, four WRF sensitivity experiments were carried out on these days to investigate the performance of the WRF model during the different seasons. Based on data availability, the WRF model is forced by the NCEP/NCAR reanalysis dataset. Two days while running the WRF simulations were recognized as a spin-up time to adequately develop mesoscale processes. The WRF model outputs were proceeding every hour with 27 pressure levels and the model top of 50 hPa. The selected WRF model physics schemes in this study are shown in Table 3. The purpose of the present work was to investigate the success and accuracy of the WRF model based on the selected physics schemes in predicting wind speed over the study area, comparable to the ground station measurements. However, for a deeper understanding of the results, it is beneficial to have some idea of the accuracy at which the model can simulate wind speed for different regions in Egypt, Sudan, and South Sudan. Thus, statistical analysis procedures were executed to compare the WRF model and observations at the selected 19 ground stations.

Table 3: Selected WRF model physics schemes.

Physics scheme	Type of the scheme that used in WRF run
Microphysics	Single-moment 3-class WSM3 scheme
Longwave radiation	Rapid Radiative Transfer Model (RRTM) scheme
Shortwave radiation	Dudhia scheme
Land surface	Noah Land Surface Model scheme
Surface and boundary layers	Yonsei University scheme
Cumulus parameterization	Kain-Fritsch scheme

Statistical analysis methods

To investigate the goodness of fit measurements between the measured and predicted wind speed for the selected stations, the following statistical analysis methods were used.

Willmott Index of agreement (WI)

Willmott has developed an index to measure the degree of difference between model predictions and observations; its value varies between 0 and 1 [43]. When the difference is 1, it represents a perfect match between the predictions and observations. While if it is 0, it indicates that there is no agreement at all. It is given by equation (1):

$$WI = 1 - \frac{\sum_{i=1}^{n}(X_i - Y_i)^2}{\sum_{i=1}^{n}(|(Y_i - \bar{X})| - |(X_i - \bar{X})|)^2} \quad (1)$$

Where X_i, and Y_i represents the observed, observed average, and simulated values respectively.

Coefficient of Determination (R^2)

The coefficient of determination is an indicator that assesses how well a model predicts projected outputs. Also, it represents the degree of variation in the dataset. R^2 value ranges between 0 and 1 because it is the square of the correlation between the modeled and measured variables. Where higher values indicate less error variance and that the model has a good fit and values greater than 0.5 are considered acceptable [44,45]. The R^2 is given by equation (2):

$$R^2 = 1 - \frac{\sum_{i=1}^{n}(X_i - Y_i)^2}{\sum_{i=1}^{n}(X_i - \bar{X})^2} \quad (2)$$

Normalized Root Mean Square Error (NRMSE)

It is considered one of the very important statistical tools which give a good overall measure of model performance. The weighting of prediction-observation by its square tends to inflate Root Mean Square Error (RMSE), particularly when extreme values are present. Concerning a perfect model, the RMSE should approach zero [46]. RMSE is normalized by dividing its values by the average observed and multiplying by 100 [47-49], this formula is given by equation (3):

$$NRMSE = \left[\sqrt{\left(\frac{1}{n}\sum_{i=1}^{n}(Y_i - X_i)^2\right)} \Big/ \bar{X}\right] * 100 \quad (3)$$

Where n represents the number of observed and predicted values used in the comparison.

Normalized Mean Bias Error (NMBE)

The Mean Bias Error (MBE) is considered to evaluate the model performance and measure the systematic error between the predicted and observed values [50]. Lower numbers are best and values less than 0 indicate under-prediction. It is also normalized by dividing its values by the average observed and multiplying by 100 (NMBE) [51]. It is given by equation (4):

$$NMBE = \left[\left(\frac{1}{n}\sum_{i=1}^{n}(Y_i - X_i)\right) \Big/ \bar{X}\right] * 100 \quad (4)$$

Results and Discussion

Figure 3 shows a comparison between measured and predicted wind speed for the selected stations during spring (26 April 1999). One may notice that the WRF model reveals a good performance and is in harmony compared to the observed wind speed at all stations during spring. But the predicted wind speed over all stations is slightly greater than the observed one (overestimations). Figure 4 shows a comparison between measured and predicted wind speed for the selected 19 stations in Egypt, Sudan, and South Sudan during winter (22 January 2010). The predicted values of wind speed using the WRF model have the same symmetry and behavior as the observed one. In addition, the difference between the predicted and observed wind speed may be reached zero over most stations. Hence, the performance of the WRF model in predicting wind speed in the winter is better than in spring. The comparison between measured and predicted wind speed for the selected stations in Egypt, Sudan, and South Sudan during summer (12 September 1989) is shown in Figure 5. It was observed that the pattern of the predicted wind speed is similar in shape and harmony with the observed one over all stations.

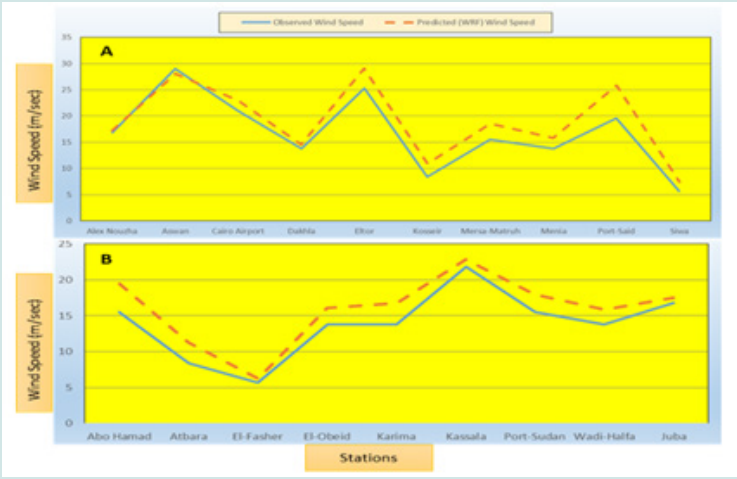

Figure 3: Comparison between measured and predicted wind speed during spring for selected stations: (A): Egypt stations, (B): Sudan, and South Sudan.

Figure 4: Comparison between measured and predicted wind speed during winter for selected stations: (A): Egypt, (B): Sudan, and South Sudan.

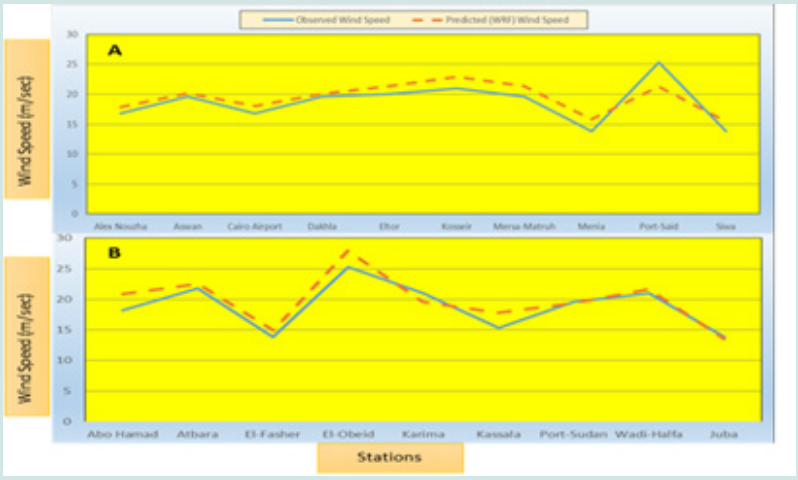

Figure 5: Comparison between measured and predicted wind speed during summer for selected stations: (A): Egypt, (B): Sudan, and South Sudan.

Figure 6 shows a comparison between measured and predicted wind speed for (A) Egypt stations, (B) Sudan, and South Sudan during autumn (7 November 2003). The predicted values of wind speed using the WRF model have the same symmetry and behavior as the observed one. In addition, the differences between the predicted and observed values are very small over most stations. Hence, the performance of the WRF model in predicting wind speed in autumn is very good and mostly like summer and winter. Therefore, the highest performance of the WRF model in predicting wind speed could be arranged from highest to lowest in summer, autumn, and winter and slightly decrease in spring. Overall, it may conclude that; Egypt, Sudan, and South Sudan can depend on the WRF model to predict wind speed in the future with high confidence. In addition, Tables 4 & 5 show small differences between measured and predicted wind speed at the selected stations. It is noticed that the WRF model wind speed average was overestimated compared to the measured one at all stations with a maximum difference in the spring season reached at above 2 m/sec. Furthermore, the comparisons between predicted and measured wind speed at each season and station have different behavior in prediction than others, but overall, the model results and prediction errors are relatively acceptable with a maximum systematic difference during the spring season.

Figure 6: Comparison between measured and predicted wind speed during Autumn for selected stations: (A): Egypt, (B): Sudan, and South Sudan.

Table 4: Measured and predicted wind speed and their difference for Egypt.

Stations	Autumn			Summer			Winter			Spring		
	X	Y	D	X	Y	D	X	Y	D	X	Y	D
Alex Nouzha	15.5	16.99	1.49	16.8	17.87	1.07	22.2	24.2	2	16.8	17.23	0.43
Aswan	19.6	22.06	2.46	19.6	20.18	0.58	16.8	15.22	-1.58	29	28.09	-0.91
Cairo Airport	12.4	12.21	-0.19	16.8	18.03	1.23	18.2	20.51	2.31	21	22.91	1.91
Dakhla	8.4	7.53	-0.87	19.6	20.07	0.47	4.1	7.02	2.92	13.8	14.57	0.77
Eltor	28	30.76	2.76	20	21.37	1.37	28	26.12	-1.88	25.3	29.05	3.75
Kosseir	22.2	19.7	2.5	21	22.91	1.91	13.8	15.27	1.47	8.4	10.91	2.51
Mersa-Matruh	16.8	17.85	1.05	19.6	21.38	1.78	23.6	22.64	-0.96	15.5	18.56	3.06
Menia	11.2	12.08	0.88	13.8	15.77	1.97	4.1	7.54	3.44	13.8	15.79	1.99
Port-Said	15.5	16.45	0.95	25.3	21.3	-4	21	22.36	1.36	19.6	25.86	6.26
Siwa	8.4	10	1.6	13.8	15.49	1.69	7.1	11.62	4.52	5.7	7.47	1.77
Average	15.8	16.56	0.76	18.63	19.44	0.81	15.89	17.25	1.36	16.89	19.04	2.15

Table 5: Measured and predicted wind speed and their difference for Sudan and South Sudan.

Stations	Autumn			Summer			Winter			Spring		
	X	Y	D	X	Y	D	X	Y	D	X	Y	D
Abo Hamad	9.8	10.2	0.4	18.2	20.88	2.68	16.8	18.41	1.61	15.5	19.48	3.98
Atbara	11.2	11.9	0.7	21.8	22.56	0.76	29.8	29.93	0.13	8.4	11.3	2.9
El-Fasher	9.8	11.19	1.39	13.8	14.96	1.16	23.6	24.92	1.32	5.7	6.24	0.54
El-Obeid	13.8	15.88	2.08	25.3	27.95	2.65	23.6	24.38	0.78	13.8	16.06	2.26
Juba	5.7	9.22	3.52	13.8	13.51	-0.29	11.2	12.95	1.75	16.8	17.55	0.75
Karima	22.2	24.87	2.67	21	19.53	-1.47	19.6	21.25	1.65	13.8	16.78	2.98
Kassala	21.8	21.85	0.05	15.3	17.78	2.48	28	27.83	-0.17	21.8	22.87	1.07
Port-Sudan	16.8	18.42	1.62	19.6	19.41	-0.19	19.6	21.66	2.06	15.5	17.95	2.45
Wadi-Halfa	21	22.61	1.61	21	21.68	0.68	13.8	14.84	1.04	13.8	15.87	2.07
Average	14.68	16.24	1.56	18.87	19.81	0.94	20.67	21.8	1.13	13.9	16.01	2.11

From a statistical point of view, the results in a Table 6 indicated that the predicted wind speed values were close to the measured ones. The goodness of fit test revealed a significant convergence between the measured and predicted values. Where R^2 and WI values are closer to 1 for all seasons except summer in Egypt, Sudan, and South Sudan. While the NRMSE values ranged from 9.715% during autumn to 16.880% during spring in Egypt and from 6.470% during winter to 17.040% during spring in Sudan. Furthermore, NMBE values simulated the same behavior of NRMSE with maximum bias during spring in Egypt, Sudan, and South Sudan with 12.755% and 15.181% respectively. These results are confirmed in Tables 4 & 5. The results in Table 6 showed that the best goodness occurred during autumn in Egypt and winter in Sudan and South Sudan. While the lowest correlation between observed and predicted wind speed was during summer in Egypt, Sudan, and South Sudan. It was noticed that there are no significant differences between the observed wind speed and the WRF forecasts during all seasons, which confirms that the WRF model success and has a good ability and high performance to simulate and predict wind speed during the different seasons over the three countries.

Table 6: Goodness of fit test between measured and predicted wind speed selected stations.

Season	Egypt Stations				Sudan and South Sudan Stations			
	WI	R^2	NRMSE	NMBE	WI	R^2	NRMSE	NMBE
Autumn	0.998	0.947	9.715	4.023	0.997	0.967	12.771	10.62
Summer	0.998	0.76	9.991	4.335	0.998	0.883	8.842	4.988
Winter	0.995	0.957	15.564	8.562	0.999	0.992	6.47	5.471
Spring	0.994	0.927	16.88	12.755	0.994	0.943	17.04	15.181

Conclusion

The WRF wind speed prediction was in harmony comparable to the observation over the study area (Egypt, Sudan, and South Sudan) with high performance during all seasons except spring. The highest values of WI and R^2 were close to 1 and the smallest ones of NRMSE and NMBE were close to zero, thus there was a strong correlation between predicted and measured wind speed. In addition, there were no significant differences between the actual and forecasted wind speed for the selected days. Therefore, the WRF model is competent to predict wind speed over Egypt, Sudan, and South Sudan. The highest performance of the WRF model was in autumn in Egypt and winter in Sudan, South Sudan, where the NRMSE values were small. While its lowest one was found in summer compared to observation due to its maximum difference and highest NRMES. Overall results proved the capability of the WRF model to predict wind speed over Egypt, Sudan, and South Sudan compared to measurements. In general, it may conclude that; Egypt, Sudan, and South Sudan can depend on the WRF model to predict wind speed in the past, present, and future with relatively high confidence and accuracy.

References

1. Huang X, Ma Y, Mills G (2008) Verification of mesoscale NWP forecasts of abrupt wind changes. Melbourne, Australia, A partnership between the Centre for Australian Weather and Climate Research and the Bureau of Meteorology. CAWCR Technical Report No. 008.
2. Randall D (2011) An Introduction to the General Circulation of the Atmosphere. Department of Atmospheric Science, Colorado State University, USA.
3. Akinyemi ML, Emetere ME, Akinwumi SA (2016) Dynamics of Wind Strength and Wind Direction on Air Pollution Dispersion. Asian Journal of Applied Sciences 4(2): 422-429.

4. Saber A, Abdel H, Morsy M, El-Hussainy FM, Eid MM (2020) Characteristics of the simulated pollutants and atmospheric conditions over Egypt. NRIAG J Astron Geophys 9(1): 402-419.
5. Barry RG, Chorley RJ (1998) Atmosphere, weather & climate, Seventh edition, London Routledge, UK.
6. Sempreviva A, Barthelmie R, Pryor S (2008) Review of methodologies for offshore wind resource assessment in European seas. Surv Geophys 29(6): 471-497.
7. Hahmann A, Rostkier-Edelstein D, Vandenberghe F, Liu Y, Swerdlin S, et al. (2010) A reanalysis system for the generation of mesoscale climatographies. J Appl Meteor Climatol 49(5): 954-972.
8. Shimada S, Ohsawa T (2011) Accuracy and characteristics of offshore wind speeds simulated by WRF Sci Online Lett Atmos 7(1): 21-24.
9. Cassola F, Burlando M (2012) Wind speed and wind energy forecast through Kalman filtering of Numerical Weather Prediction model output. Appl Energy 99: 154-66.
10. Chen Z (2013) Wind power in modern power systems. J Mod Power Syst Clean Energy 1(1): 2-13.
11. Draxl C (2012) On the Predictability of Hub Height Winds. DTU Wind Energy. Risø.
12. Lazić L, Pejanović G, Živković M, Ilić L (2014) Improved wind forecasts for wind power generation using the Eta model and MOS (model output statistics) method. Energy 73(7): 567-574.
13. Santhosh M, Venkaiah C, Kumar DMV (2020) Current advances and approaches in wind speed and wind power forecasting for improved renewable energy integration: A review. Engineering Reports 2(2): 20.
14. Zhang J, Draxl C, Hopson T, Monache LD, Vanvyve E, et al. (2015) Comparison of numerical weather prediction based deterministic and probabilistic wind resource assessment methods. Appl Energy 156(11): 528-541.
15. Nie Y, Bo H, Zhang W, Zhang H (2020) Research on Hybrid Wind Speed Prediction System Based on Artificial Intelligence and Double Prediction Scheme. Complexity 1: 22.
16. Weekes S, Tomlin A (2013) Evaluation of a semi-empirical model for predicting the wind energy resource relevant to small-scale wind turbines. Renewable Energy 50: 280-288.
17. Chang TP (2011) Performance comparison of six numerical methods in estimating Weibull parameters for wind energy application. Appl Energy 88(1): 272-82.
18. Standen J, Wilson C, Vosper S, Clark P (2017) Prediction of local wind climatology from met office models: virtual met mast techniques. Wind Energy 20(3): 411-430.
19. Santos-Alamillos FJ, Pozo-Vazquez D, Ruiz-Arias JA, Vicente L F (2013) Analysis of WRF Model Wind Estimate Sensitivity to Physics Parameterization Choice and Terrain Representation in Andalusia (Southern Spain). J Appl Meteor Climatol 52(7): 1592-1609.
20. Allena DJ, Tomlinb AS, Baleb CSE, Skea A, Vosper S, et al. (2017) A boundary layer scaling technique for estimating near-surface wind energy using numerical weather prediction and wind map data. Appl Energy 208: 1246-1257.
21. Maurizi A, Palma JM, Castro FA (1998) Numerical simulation of the atmospheric flow in a mountainous region of the North of Portugal. J. Wind Eng. Ind. Aerodyn 74-76: 219-228.
22. Mcqueen D, Watson S (2006) Validation of wind speed prediction methods at offshore sites. Wind Energy 9(1-2): 75-85.
23. Finardi S, Tinarelli G, Faggian P, Brusasca G (1998) Evaluation of different wind field modeling techniques for wind energy applications over complex topography. J Wind Eng Ind Aerodyn 74-76: 283-294.
24. Conte A, Pavone A, Ratto CF (1998) Numerical evaluation of the wind energy resource of Liguria. J Wind Eng Ind Aerodyn 74-76: 355-364.
25. Beaucage P, Glazer A, Chosinard J, Yu W, Bernier M, et al. (2007) Wind assessment in a coastal environment using synthetic aperture radar satellite imagery and a numerical weather prediction model. Can J Remote Sens 33(5): 368-377.
26. Miglietta MM, Rotunned R (2009) Numerical simulations of conditionally unstable flows over a mountain ridge. J Atmos Sci 66(7): 1865-1885.
27. Skamarock WC, Klemp JB, Jimy D, Gill DO, Dale B et al. (2008) A description of the Advanced Research WRF version 3. NCAR Tech Rep, pp. 113.
28. De Jong P, Dargaville R, Silver J, Utembe S, Kiperstok A, et al. (2017) Forecasting high proportions of wind energy supplying the Brazilian Northeast electricity grid. Appl Energy 195(19): 538-55.
29. Carvalho D, Rocha A, Santos CS, Pereira R (2013) Wind resource modelling in complex terrain using different mesoscale-microscale coupling techniques. Appl Energy 108: 493-504.
30. Kibona TE (2020) Application of WRF mesoscale model for prediction of wind energy resources in Tanzania. Scientific African 7: e00302.
31. Yu W, Benoit R, Girard C, Glazer A, Lemarquis D, et al. (2006) Wind energy simulation toolkit (WEST): A wind mapping system for use by the wind-energy industry. Wind Eng 30(1): 15-33.
32. Draxl C, Hahmann AN, Peña A, Giebel G (2014) Evaluating winds and vertical wind shear from weather research and forecasting model forecasts using seven planetary boundary layer schemes. Wind Energy 17(1): 39-56.
33. Giannakopoulou E-M, Nhili R (2014) WRF model methodology for offshore wind energy applications. Adv Meteorol p. 9.
34. Penchah MM, Malakooti H, Satkin M (2017) Evaluation of planetary boundary layer simulations for wind resource study in East of Iran. Renew Energy 111: 1-10.
35. Carvalho D, Rocha A, Gómez-Gesteira M, Santos CS (2014) sensitivity study of the WRF model in wind simulation for an area of high wind energy. Environ Modell Softw 33: 23-34.
36. Skamarock WC (2004) Evaluating mesoscale NWP models using kinetic energy spectra. Mon Weather Rev 132(12): 3019-3031.
37. Hemanth MB, Saravanan B, Sanjeevikumar P, Jens H-N (2019) Wind Potential Assessment by Weibull Parameter Estimation Using Multiverse Optimization Method: - A Case Study of Region in India. Energies 12(11): 1-21.
38. Carvalho D, Rocha A, Gómez-Gesteira M, Santos CS (2014) WRF wind simulation and wind energy production estimates forces by different reanalyses: Comparison with observed data for Portugal. Appl Energy 117: 116-126.
39. Sandeepan BS, Panchang VG, Nayak S, Kumar KK, Kaihatu JM (2018) Performance of the WRF Model for Surface Wind Prediction around Qatar. J Atmos Oceanic Technol 35(3): 575-592.
40. Chadee XT, Seegobin NR, Clarke RM (2017) Optimizing the Weather Research and Forecasting (WRF) Model for Mapping the Near-Surface Wind Resources over the Southernmost Caribbean Islands of Trinidad and Tobago. Energies 10(7): 931.
41. Nicholls SD (2012) Impact of four WRF modifications upon eight nor'easter simulations. New Brunswick Graduate School, Rutgers, New Jersey, State University, USA.
42. Wireman CS (2012) Evaluation of non-convective wind forecasting methods in the 15th operational weather squadron area of responsibility. Naval postgraduate school, Captain, United States Air Force.

43. Willmott CJ (2013) On the validation of models. Physical Geography 2: 184-194.

44. Van Liew MW, Arnold JG, Garbrecht JD (2003) Hydrologic simulation on agricultural watersheds: Choosing between two models. Trans ASAE 46(6): 1539-1551.

45. Moriasi DN, Arnold JG, Van Liew MW, Bingner RL, Harmel RD, et al. (2007) Model evaluation guidelines for systematic quantification of accuracy in watershed simulations. Trans ASABE 50(3): 885-900.

46. El Afandi G, Morsy M, El Hussieny F (2013) Heavy Rainfall Simulation over Sinai Peninsula Using the Weather Research and Forecasting Model. Int J Atmos Sci 1: 241050.

47. Mentaschi L, Besio G, Cassola G, Mazzino A (2013) Developing and validating a forecast/hindcast system for the Mediterranean Sea, Proceedings 12th International Coastal Symposium (Plymouth, England). J Coast Res 65(65): 1551-1556.

48. Sarkalkan N, Loeve A, Dongen K, Tuijthof G, Zadpoor A (2015) A Novel Ultrasound Technique for Detection of Osteochondral Defects in the Ankle Joint: A Parametric and Feasibility Study. Sensors 15: 148-165.

49. Taebi A, Mansy HA (2017) Time-Frequency Distribution of Seismocardiographic Signals: A Comparative Study. Bioengineering 4(2): 32.

50. Singh AK, Goyal V, Mishra AK, Parihar SS (2013) Validation of Crop Syst simulation model for direct seeded rice-wheat cropping system. Current science 104(10): 1324-1331.

51. Sayad T, Ouda S, Morsy M, El Hussieny F (2015) Robust statistical procedure to determine suitable scenario of some CMIP5 models for four locations in Egypt. Glob J Adv Res 2(6): 1009-1019.

DOI: 10.32474/JBRS.2022.02.000134